

Optical pump–terahertz probe spectroscopy of dyes in solutions: Probing the dynamics of liquid solvent or solid precipitate?

Filip Kadlec, Christelle Kadlec, and Petr Kužel

Institute of Physics, Academy of Sciences of the Czech Republic and Center for Complex Molecular Systems and Biomolecules, Na Slovance 2, 18221 Prague 8, Czech Republic

Petr Slavíček and Pavel Jungwirth

J. Heyrovský Institute of Physical Chemistry, Academy of Sciences of the Czech Republic and Center for Complex Molecular Systems and Biomolecules, Dolejškova 3, 18223 Prague 8, Czech Republic

(Received 22 September 2003; accepted 17 October 2003)

The optical pump–terahertz probe spectroscopy was used together with *ab initio* calculations and molecular dynamics simulations to investigate ultrafast dynamics following electronic excitation of Coumarin 153 and TBNC (2,11,20,29-tetra-*tert*-butyl-2,3-naphthalocyanine) dyes in polar solvents. By scanning the terahertz waveform for different pump–probe delays this experimental technique allows us to obtain two dimensional spectra directly reflecting the temporal response of the system. A distinct signal was obtained for TBNC in chloroform, 2-propanol, and *n*-butanol, while no signal was recorded for Coumarin 153 in either of these solvents. We explain the nonequilibrium signal detected in TBNC solutions by the presence of a solid, polycrystalline phase of the dye resulting from irradiating the solution by intense optical pulses. © 2004 American Institute of Physics. [DOI: 10.1063/1.1633256]

I. INTRODUCTION

The role of solvent in liquid phase chemical processes can hardly be overstated. Consequently, a considerable experimental and theoretical effort has been directed towards elucidating the solute–solvent and solvent–solvent interactions and dynamics, preferably at a molecular level of resolution. In particular, solvent relaxation following excitation of the solute plays an important role in liquid state photochemistry, electron and proton transfer, and other chemical processes. Provided that the dynamical perturbation of the solvent by solute excitation is weak the linear response approach can be invoked. This basically means that the solvent response is independent of the particular solute and is directly related to thermal fluctuations of the neat solvent via the Onsager regression hypothesis and the fluctuation–dissipation theorem.¹ A large body of time-resolved spectroscopic studies, as well as molecular dynamics (MD) simulations have been directed to investigations of weakly perturbed solvents. As a result, the relaxation dynamics of many polar and nonpolar liquids in or near the linear response regime is well characterized today.^{2–6}

Much less is known about a nonlinear solvent response to a strong perturbation by a large change in electronic structure and/or geometry of the solute due to electronic excitation.⁷ In the nonlinear regime a particular solvent responds specifically to different solutes and the simple relation between the nonequilibrium response function and the equilibrium autocorrelation function¹ does not hold any more. It has been shown recently that although most of the chemical processes in solvents probably fall into the linear response regime, there are important exceptions involving, e.g., solvent response to a simultaneous change in charge distribution and geometric shape of the solute. This can have

significant consequences for liquid state chemistry, in particular for charge-transfer reactions.^{7,8}

While solute electronic excitations typically occur in the visible or ultraviolet region of the spectrum, the librational, rotational, and translational response of the solvent correlates with the far-infrared (terahertz) spectral region. For this reason, the optical pump–terahertz probe (OPTP) spectroscopy seems to be ideally suited for studying solvent relaxation on the picosecond time scale. Experiments for Betaine 30, *p*-nitroaniline, and TBNC (2,11,20,29-tetra-*tert*-butyl-2,3-naphthalocyanine) in polar solvents such as chloroform have been performed so far.^{9–13} Within this technique an optical femtosecond pulse is used to excite the solute, while a terahertz (THz) ultrashort pulse probes directly the subsequent solvent relaxation. On the one hand, there are several advantages to the OPTP technique: it probes in the most relevant frequency region and, thus, it should be particularly sensitive to nonlinear nonequilibrium processes. Moreover, it provides a phase-sensitive information in the whole THz range (i.e., roughly 1–100 cm⁻¹). On the other hand, solvents typically exhibit only weak nonequilibrium variations in THz absorbance (unlike semiconductors, where the OPTP method is routinely used^{14–17}). Moreover, interpretation of changes in the THz waveform caused by the temporal evolution of the system requires a very careful analysis due to frequency mixing.^{18–20}

This paper presents results of OPTP experiments and simulations of two dyes, Coumarin 153 (C153) and TBNC in chloroform and other polar solvents. Coumarins, which have been widely used as probes of picosecond solvent dynamics,^{21,22} exhibit a large change of dipole moment upon electronic excitation. Consequently, a strong response of the polar solvent can be expected. TBNC is less polar than Cou-

marin 153 and the variation of its electronic density between the ground and electronically excited state is also weaker.¹² Nevertheless, a distinct OPTP signal has been recorded for TBNC in chloroform and toluene.^{11–13} The principal goal of the present study is to analyze the OPTP spectra in terms of the underlying molecular dynamics. In particular, we aim at distinguishing solvent contributions from those of the dyes. The rest of the paper is organized as follows. The experimental setup is described in detail in Sec. II. The systems under investigation, together with computational approaches are presented in Sec. III. Section IV contains the experimental results and discussion thereof, while results of calculations are summarized in Sec. V. Finally, concluding remarks can be found in Sec. VI.

II. EXPERIMENTAL SETUP

The experimental setup is similar to that described in Ref. 12. As a light source, we used a Quantronix Odin Ti:sapphire multipass femtosecond pulse amplifier producing ≈ 60 fs, 815 nm laser pulses with an energy about 1 mJ and a repetition rate 1 kHz. The pulses are split into three branches, all of them including delay lines for a precise control of pulse arrival times. About one third of the power is used for optically pumping the sample (pump branch), either directly or using a second harmonic generation in a LBO crystal, which yields typically 40 μ J pulses at 407 nm. The second part of the pulses (probe branch) generates the THz probe radiation via optical rectification in a 1 mm thick [011] ZnTe crystal. The radiation is focussed onto the sample using an ellipsoidal mirror, leading to a peak electric field of the order of units of kV/cm. The third part of the pulse (sampling branch) is strongly attenuated and used for sampling the transmitted THz field using the electro-optic effect in another [011] ZnTe crystal.

A lock-in amplifier and a chopper operating at 166 Hz are used for the synchronous detection. The THz electric field intensity $E(t)$ transmitted through the sample in equilibrium (without optical pumping) can be acquired if the chopper is placed into the probe branch. If the chopper is moved into the pump branch, photoinduced changes in the THz waveform $\Delta E(t, t_e)$ are detected (t_e defines the pump beam arrival).

A great care has been taken to optimize the signal-to-noise ratio and the dynamic range of the measurements. The noise can be significantly reduced by performing multiple scans of the delay lines and data averaging. The dynamic range in the time domain characterizes the smallest detectable signal ΔE with respect to the maximum equilibrium signal. Taking into account the temporal stability of the whole setup, we achieve the ratio $\Delta E/E \lesssim 10^{-5}$, which corresponds to 10 orders of magnitude dynamic range in power. The typical performance in the frequency domain is shown in Fig. 1.

The sample is a solution of C153 or TBNC in chloroform, 2-propanol or *n*-butanol. These polar solvents are chosen since they exhibit a low absorption coefficient in the THz range and the walk-off²⁰ between optical and THz pulses is low. About 100–200 ml of the solution are pumped through a 1 mm flow cuvette with 1.25 mm thick infrasil windows.

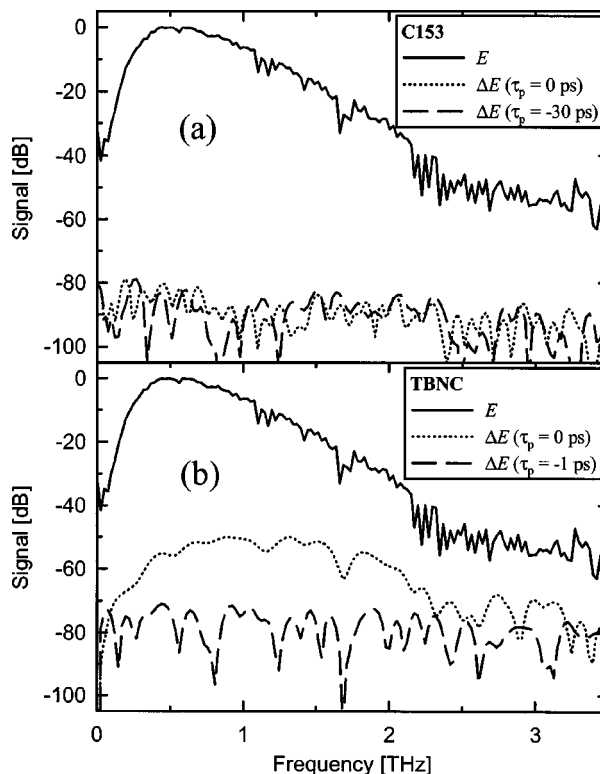


FIG. 1. The spectral sensitivity of the THz spectrometer as obtained (a) for Coumarin 153, and (b) for TBNC in chloroform, with a 30 ms detection time base. The equilibrium spectrum E was measured in a single scan, while the OPTP data ΔE were obtained from 160 scans (Coumarin 153) and 30 scans (TBNC). The dashed line indicates the noise level of time-resolved measurements for the given numbers of scans.

At the typical pump rate of about 0.5 l/min, the active sample volume is completely renewed within three pulses. The angle of incidence of the pump pulse on the sample with respect to the direction of the probe pulse is about 10° , which limits the time resolution to 1 ps. A circular 3 mm diaphragm is placed behind the cuvette, so that the cross section of the excited volume (about 20 mm²) is larger than that of the probed volume. A spatial profile of the pump beam may possibly induce weak lensing of the THz beam. This may change its spatial properties and thus enhance or reduce slightly the detected transient signal ΔE . However, the build-up and decay of such a lens is caused by the induced changes of the complex refractive index of the sample which directly reflect the investigated dynamics. Thus, no artificial dynamical signal can originate from possible lensing.

III. SYSTEMS AND COMPUTATIONAL METHODS

We have explored the possibility to simulate the optical pump–terahertz probe experiment by means of molecular dynamics. The first step is to generate an equilibrium ensemble sampling the distribution at an experimental temperature. Then, at time t_e the potential parameters of the solute change instantaneously, accounting for the dye excitation. For convenience, we set $t_e=0$ in the simulations. We have employed the following three computational approaches to follow the subsequent dynamics.

The direct simulation of the experiment means that at time t_p the probe pulse is applied and, finally, at time $t > t_p$ the polarization $M(t, t_p)$ is recorded. Providing that the probing pulse is of a delta shape, the polarization of the sample is actually the measured response function $\chi(t, t_p)$. This straightforward approach is, however, not computationally feasible. This is since in the simulation the signal-to-noise ratio for experimentally accessible probe fields is highly unfavorable.

This brings us to the second possibility which is to calculate a two dimensional correlation function $C(t, t_p) = M(t_p)M(t)$. The difference between this two dimensional correlation function $C(t, t_p)$ and the equilibrium (one dimensional) correlation function $C(t)$ contains the information about the nonequilibrium dynamics. However, for nonequilibrium situation no direct analogue of the fluctuation-dissipation theorem connecting the correlation function and the response function of the system exists. Thus, the two dimensional correlation function cannot be directly linked to the experimental observables.

Finally, one can also get an insight into the experiment by instantaneous normal modes (INM) analysis²³ of the non-equilibrium ensemble. Briefly, by diagonalizing the Hessian at a given instantaneous position generated using the MD simulation, and by subsequent histogramming of the frequencies we get the transient harmonic density of states. As in Ref. 24 the density of states is weighted by the corresponding change in dipole moment. This approach can be used for the description of short time dynamics of liquids and it has been employed, e.g., to calculate the dielectric properties of liquids under equilibrium conditions.²⁴ Under nonequilibrium conditions, one can calculate the time resolved vibrational density of states $\rho(\omega, t)$ which in general differs from that of an equilibrium system $\rho(\omega)$. Note that in the experiment only those frequencies can be observed which survive in the calculated “snapshot” density of states $\rho(\omega, t)$ longer than the vibrational period of the given mode.

Both the simulations of two dimensional correlation function and the INM density of states still suffer from significant noise since the nonlinear effects are generally very small. To suppress it we have recorded the signal only from solvent molecules residing in a cavity surrounding the solute. This is straightforward in the case of the two dimensional correlation functions. In the case of INM density of states we can realize the cavity by projecting the normal modes onto a specific spatial region using the eigenvectors of the Hessian.

We simulated the solvation dynamics in chloroform of the Coumarin 151 (C151) dye, which is very similar to the experimentally investigated C153 dye, and for which potential parameters exist in the literature. The force field for C151 was taken from Ref. 25, while the parameters for chloroform were adopted from Ref. 26. In the simulation, a single C151 molecule was dissolved in a box of 200 chloroform molecules. Within this arrangement we avoided complexation or even precipitation of the dye. In addition we also simulated a model homonuclear diatomic molecule in SPCE water.²⁷ The van der Waals parameters of the atoms of the diatomics were $\sigma = 4.6 \text{ \AA}$ and $\epsilon = 0.1 \text{ kcal/mol}$. The equi-

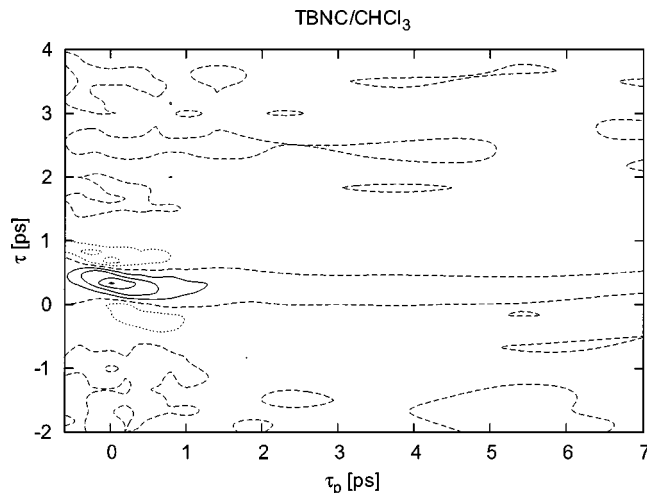


FIG. 2. Optical pump–terahertz probe data obtained from a two dimensional scan of a 2 mM solution of TBNC in chloroform. Solid lines, positive contours; dashed lines, zero level contours; dotted lines, negative contours.

librium diatomic bondlength was 2.56 \AA and the atoms possessed partial charges of $\pm 0.5e$.

In connection with the second experiment presented in this study, we have investigated the nature of phthalocyanine and naphthalocyanine in the ground and first electronically excited states, as well as TBNC in the ground state. We have calculated the optimal geometry at the Hartree–Fock level using the 3-21g basis set. At this geometry, we have calculated the vertical excitation energies, dipole moments in the ground and excited states (which for phthalocyanine and naphthalocyanine possess different symmetries), and the molecular polarizabilities. Finally, we have performed an optimization of the excited state geometry at the same level, preserving the system symmetry during the calculation.

IV. EXPERIMENTAL RESULTS

A solution of TBNC in chloroform with a concentration of 2 mM was studied in considerable detail. The signal amplitude for this experiment was $\Delta E_{\max}/E_{\max} \approx 0.003$, i.e., about two orders of magnitude above the noise level [see Fig. 1(b)]. We have performed two dimensional scans according to the methodology described earlier.²⁰ The pump pulse arrives at t_e , the probe pulse arrival is connected to the time t_p , and the delay line in the sampling branch allows scanning the shape of the freely propagating THz waveforms (time t). In our experiments we scanned the delay lines in the pump (t_e) and sampling (t) branches. Similarly as in Ref. 20, we define the delay times $\tau_p = t_p - t_e$ and $\tau = t - t_p$. The contour plot of the measured data is shown in Fig. 2. The coordinate τ_p thus denotes the pump–probe delay and the τ scans yield the nonequilibrium part of the waveform propagating between the sample and the sensor for a given pump–probe delay. Similarly to results published in Ref. 12, one can see in Fig. 2 that the signal has a shape elongated along the coordinate corresponding to the pump–probe delay time τ_p . The signal has apparently two components, a fast (picosecond) one and a slow one, which decays within 100 ps.

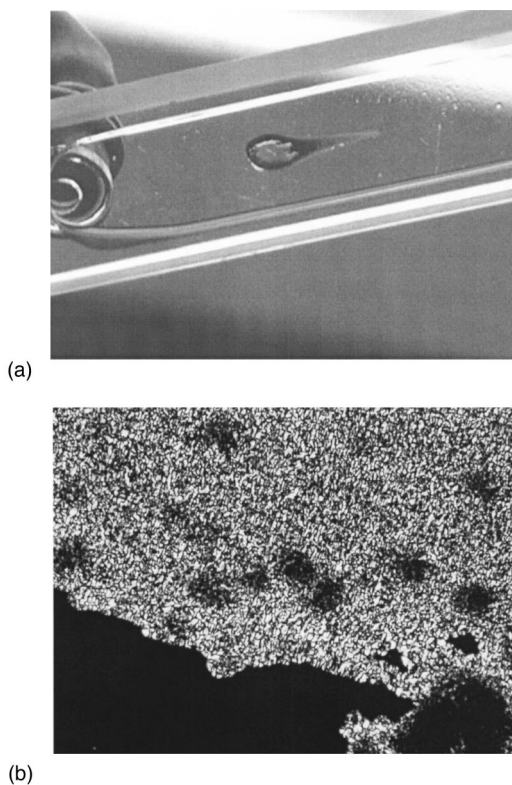


FIG. 3. (a) A view of the cuvette with the polycrystalline phase created by exposing the TBNC/chloroform solution to near-infrared light pulses. (b) A polarizing microscope view of the layer displayed in (a). The picture width corresponds to ≈ 1 mm.

We have observed that, during the measurements, a solid layer of TBNC appears on the inner surface of the cuvette input window in the place where the sample is irradiated by the excitation pulse. Since the dye concentration is relatively high, the solution is opaque and the layer can hardly be seen by naked eye. However, it becomes visible as soon as the solution is drained from the cuvette [see Fig. 3(a)]. A picture taken under an optical microscope clearly shows a polycrystalline phase of solid TBNC [see Fig. 3(b)]. When the cuvette is flowed again and the pump beam is blocked, the layer is washed away after a few seconds, but it appears again as soon as the pump beam is open. This suggests the idea that the OPTP signal is in some way related to the presence of this solid phase and not to solvation dynamics of single molecules. This is further supported by the fact that upon reducing the energy of pump pulses to 50%, the signal decreases roughly by a factor of 4, which is contrary to the expectation that the solvent signal should scale linearly with the pump power.²⁰ We note that at lower pump power, the solid layer becomes difficult to see even when the cuvette is drained of the liquid, which may be the reason why the solid phase has not been noticed before.

A conclusive evidence about the origin of the measured signal would be brought by performing the OPTP measurement of the solid precipitate only. However, without the circulating solvent the applied optical pump beam causes an irreversible degradation of the precipitate. Therefore, as a control experiment, we made a comparison of chosen τ scans for a series of TBNC/chloroform solutions with concentra-

tions of 2, 1, 0.5, 0.25, and 0.125 mM. Note that these concentrations are lower than those used in Ref. 12. The shape of the measured curves is essentially the same at all concentrations, except for scaling factors. The molar extinction coefficient ϵ at $\lambda=815$ nm has been determined using the Beer–Lambert law as $\epsilon=100$ $\text{mM}^{-1} \text{cm}^{-1}$. The walk-off between the THz and optical pulses in chloroform amounts to $\Delta w \approx 0.2$ ps mm^{-1} . Therefore, one would expect, if the signal came from solvation within the liquid, the signal intensity to be constant between 2 and 0.25 mM and to drop by about 40% for the lowest concentration [see Fig. 4(c) in Ref. 20]. Instead, we observe small and rather erratic variations in the signal intensity with TBNC concentration. At the same time, with decreasing concentration, the solid layer becomes more persistent and difficult to wash away. For a concentration of 0.125 mM, the signal is one of the highest in the series. We can rationalize this by the fact that at this concentration the linear absorption coefficient $\alpha=1.25$ mm^{-1} , which is a low enough value for a substantial part of the incident power to penetrate the whole cuvette. Consequently, the solid layer is observed also on the output cuvette window. Yet another argument for the solid state interpretation of the OPTP spectra is our observation of quantitatively similar spectra of TBNC in a rather different solvent—butanol. Here, the creation of the solid layer of TBNC on the cuvette window has also been recorded, even though, at the same optical power, the layer is clearly thinner and more difficult to see. We agree with the conclusion of previous work that the decay of the OPTP signal of TBNC is almost independent of the particular solvent.²⁸ However, based on the arguments given above we newly interpret the spectra of TBNC as a signal from the crystalline solute precipitate. In a sense, we may have thus unintentionally discovered a way to record the transient OPTP spectrum of solid TBNC without burning the sample by the intense optical pump pulses.

In contrast, no OPTP signal exceeding the noise level has been detected in solutions of C153 in chloroform, propanol, or butanol at 0.5 mM, using optical excitation at 407 nm. As an example, Fig. 1(a) shows data measured at two pump–probe delays: $\tau_p=0$ ps, where one could expect a signal maximum, and $\tau_p=-30$ ps, where the pump pulse comes after the sampling, so that in principle no OPTP signal can be measured, which demonstrates the lack of signal above noise level. We have also verified the signal absence at a higher concentration, in a 22 mM solution of C153 in butanol with 50 μJ pulses.

V. CALCULATIONS

In Fig. 4 we present the calculated nonlinear signal of Coumarin 151 solvated in chloroform. We display the mean square deviation between the two-time correlation function (see Sec. III) and the equilibrium correlation function $I(t_p) = \int_0^\infty (C(t, t_p) - C(t))^2 dt$ as a function of the pump–probe delay time. The signal, which is mainly due to solute dynamics, levels off after some 5 ps. This reflects the establishment of a new equilibrium pertinent to the photoexcited solute. We can thus obtain information on the time scale at which the nonlinear solvation effects play role, the frequency decom-

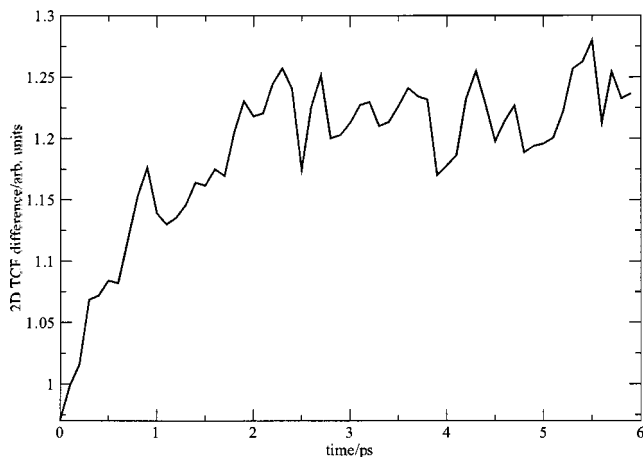


FIG. 4. Integrated difference between the two time correlation function and the equilibrium correlation function $I(t_p) = \int_0^\infty (C(t, t_p) - C(t))^2 dt$ as a function of the delay time.

position, however, is not possible. We note that the signal is extremely noisy, although we have collected the signal only from a small cavity around the solute. If we consider the response from the whole simulation box (i.e., Coumarin 151 and 216 solvents molecules), the signal is completely hidden in the noise even for a statistics from over 1000 replicas of the system.

Another way to monitor the dynamics in the excited state is to apply the INM concept, described in Sec. III. In Fig. 5 we present the time evolution of the difference between transient and equilibrium densities of state collected for the Coumarin 151 dye and surrounding small cavity of chloroform molecules. Namely, we display the data for 0, 1, and 4.5 ps pump–probe delays. Clearly, the signal for Coumarin 151 in chloroform is very noisy and the dynamical information is almost completely buried in the noise. This again correlates with the experimental problem of recording any spectra above the noise level. Note that the steady feature at around 150 cm^{-1} reflects a soft solute mode, which exhibits different transition dipole moments in the ground

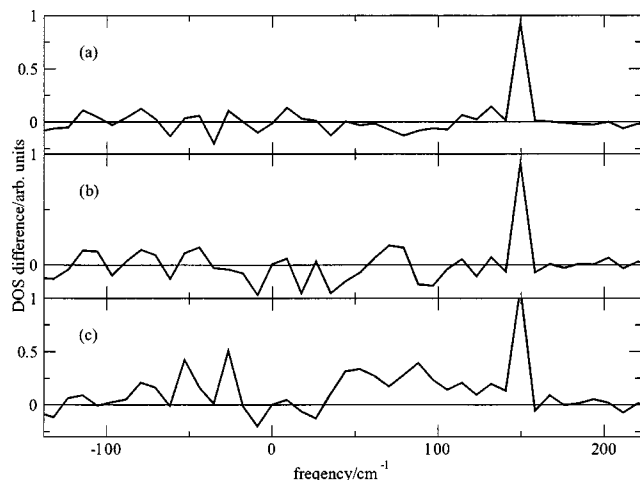


FIG. 5. The difference between transient and equilibrium densities of states of Coumarin 151 in chloroform from the instantaneous normal mode analysis for pump–probe delays of (a) 0 ps, (b) 1 ps and (c) 4.5 ps.

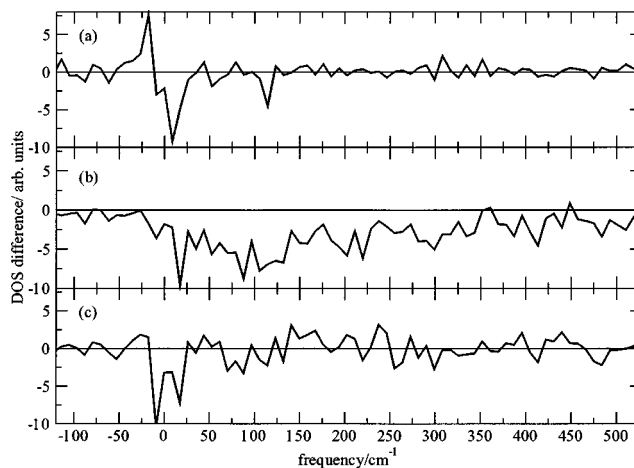


FIG. 6. The difference between transient and equilibrium densities of states of a model diatomic in water from the instantaneous normal mode analysis for pump–probe delays of (a) 0 ps, (b) 180 fs, and (c) 750 fs.

and excited electronic states. In contrast, we show in Fig. 6 similar graphs for a model system of a polar homonuclear diatomic molecule in water. The dynamics in this system is evoked by an instantaneous reversal of the polarity of the diatomic. For this aqueous system, the dynamical response emerges above the noise level and the curves for 0, 180, and 750 fs clearly differ from each other. More precisely, the 180 fs curve shows transient changes particularly in the low energy (translational and rotational) part of the spectrum, while the 750 fs signal displays already convergence towards the equilibrium (zero signal). This proves that the INM computational strategy is able to provide information about the nonlinear solvent relaxation dynamics on the subpicosecond and picosecond time scale. Also, there is good hope that a future OPTP experiment might be successful in monitoring solvent relaxation of aqueous solutions of polar dyes with a large change in dipole moment (and possibly also geometry) upon electronic excitation.

In connection with the OPTP experiments of TBNC in chloroform, we have calculated the electronic properties of a series of cyanines: phthalocyanine, naphthalocyanine, and TBNC. All three molecules have very similar properties in the electronic ground state. The ground state of these species has a dipole moment ranging from 5 to 7 D, while in the excited state (of phthalocyanine and naphthalocyanine) it is less than 1 D. The electronic excitation is also accompanied by a significant change in polarizability. For phthalocyanine, e.g., the mean polarizability raises from 71 \AA^3 in the ground state to the 99 \AA^3 in the excited state. We can thus expect enhanced clustering due to van der Waals interactions upon the electronic excitation of the molecule.

VI. CONCLUSIONS

We have performed optical pump–terahertz probe experiments for TBNC and Coumarin 153 in chloroform, 2-propanol, and *n*-butanol. A two dimensional spectrum has been recorded for TBNC in all three solvents, while no signal above the noise level was obtained for C153. The spectrum of TBNC in chloroform is similar to that obtained pre-

viously. However, in contrast to earlier investigators, we newly interpret the spectrum as originating from a polycrystalline precipitate of the TBNC dye. The experimental conclusions are further supported by two dimensional correlation functions and instantaneous normal modes obtained from molecular dynamics simulations, as well as by results of quantum chemistry calculations of the cyanite dyes.

ACKNOWLEDGMENTS

Numerous discussions with Burkhard Schmidt from FU Berlin are gratefully acknowledged. We also thank Charles Schmittenmaer from Yale University for valuable comments. This research was supported by the Volkswagen Stiftung (Grant No. I/75908) and the Czech Ministry of Education (Grant No. LN00A032).

- ¹D. Chandler, *Introduction to Modern Statistical Mechanics* (Oxford University Press, Oxford, 1987).
- ²R. Jimenez, G. R. Fleming, P. V. Kumar, and M. Maroncelli, *Nature* (London) **369**, 471 (1994).
- ³J. C. Owrutsky, D. Raftery, and R. M. Hochstrasser, *Annu. Rev. Phys. Chem.* **45**, 519 (1994).
- ⁴R. M. Stratt and M. Maroncelli, *J. Phys. Chem.* **100**, 12981 (1996).
- ⁵B. M. Ladanyi and M. Maroncelli, *J. Chem. Phys.* **109**, 3204 (1998).
- ⁶P. L. Geissler and D. Chandler, *J. Chem. Phys.* **113**, 9759 (2000).
- ⁷D. Aherne, V. Tran, and B. J. Schwartz, *J. Phys. Chem. B* **104**, 5382 (2000).
- ⁸E. R. Barthel, I. B. Martini, and B. J. Schwartz, *J. Phys. Chem. B* **105**, 12230 (2001).
- ⁹G. Haran, W.-D. Sun, K. Wynne, and R. M. Hochstrasser, *Chem. Phys. Lett.* **274**, 365 (1997).

- ¹⁰R. McElroy and K. Wynne, *Phys. Rev. Lett.* **79**, 3078 (1997).
- ¹¹D. S. Venables and C. A. Schmittenmaer, in *Ultrafast Phenomena XI*, edited by W. Zinth, J. G. Fujimoto, T. Elsaesser, and D. Wiersma (Springer, Berlin, 1998).
- ¹²M. C. Beard, G. M. Turner, and C. A. Schmittenmaer, in *ACS Symposium Series 820*, edited by J. T. Fourkas (ACS, Washington, DC, 2002).
- ¹³M. C. Beard, G. M. Turner, and C. A. Schmittenmaer, *J. Phys. Chem. B* **106**, 7146 (2002).
- ¹⁴M. C. Nuss, D. H. Auston, and F. Capasso, *Phys. Rev. Lett.* **58**, 2355 (1987).
- ¹⁵P. N. Saeta, J. F. Federici, B. I. Greene, and D. R. Dykar, *Appl. Phys. Lett.* **70**, 1477 (1992).
- ¹⁶M. C. Beard, G. M. Turner, and C. A. Schmittenmaer, *Phys. Rev. B* **62**, 15764 (2000).
- ¹⁷M. C. Beard, G. M. Turner, and C. A. Schmittenmaer, *J. Appl. Phys.* **90**, 5915 (2001).
- ¹⁸J. T. Kindt and C. A. Schmittenmaer, *J. Chem. Phys.* **110**, 8589 (1999).
- ¹⁹M. C. Beard and C. A. Schmittenmaer, *J. Chem. Phys.* **114**, 2903 (2001).
- ²⁰H. Nemeč, F. Kadlec, and P. Kuzel, *J. Chem. Phys.* **117**, 8454 (2002).
- ²¹C. F. Chapman, R. S. Fee, and M. Maroncelli, *J. Phys. Chem.* **99**, 4811 (1995).
- ²²M. L. Horng, J. A. Gardecki, and M. Maroncelli, *J. Phys. Chem. A* **101**, 1030 (1997).
- ²³T. Keyes, *J. Phys. Chem. A* **101**, 2921 (1997).
- ²⁴J. T. Kindt and C. A. Schmittenmaer, *J. Chem. Phys.* **106**, 4389 (1997).
- ²⁵A. Tarnashiro, J. Rodriguez, and D. Laria, *J. Phys. Chem. A* **106**, 215 (2002).
- ²⁶W. Dietz and K. Heinzinger, *Ber. Bunsenges. Phys. Chem.* **88**, 543 (1984).
- ²⁷H. J. C. Berendsen, J. R. Grigera, and T. P. Straatsma, *J. Phys. Chem.* **91**, 6269 (1987).
- ²⁸C. A. Schmittenmaer, *Book of Abstracts of the Centennial Meeting of the APS* (APS, Atlanta, 1999).